

Which Rope Breaks? A Study of Tension Distribution in Multi-Rope Systems

Amir Eskandari-asl^{1,*} and Roberto De Luca¹

¹*Dipartimento di Fisica “E.R. Caianiello”, Università degli Studi di Salerno, I-84084 Fisciano (SA), Italy*

We investigate the tension distribution in systems of mass-less ropes under different loading conditions. For a two-rope system, we demonstrate how the breaking scenario depends on the applied force dynamics: rapid pulling causes the lower rope to break, while gradual pulling leads to upper rope failure. Extending to a three-rope Y-shaped configuration, we identify a critical angle $\theta_C = 60^\circ$ that determines which rope breaks first. When the angle between the upper ropes exceeds this critical value, the upper ropes fail before the lower one. We further analyze how an attached mass at the junction point modifies this critical angle and establish maximum mass limits for valid solutions. Our results provide practical insights for introductory physics students understanding static forces and system stabilities.

I. INTRODUCTION

The study of tension and stability in ropes, beyond its practical importance which motivates extensive research works [1–5], offers an engaging entry point for introducing students to fundamental principles of classical mechanics, particularly Newton’s laws and force balance. Simple rope configurations can reveal complex behaviors that challenge intuition and prompt deeper investigation into the role of dynamics and geometry in force distribution.

In this paper, we analyze two common configurations: a vertical two-rope system and a Y-shaped three-rope system. These setups, while conceptually accessible, yield rich physical insights when carefully examined, and help the students overcome some difficulties in understanding basic concepts [6]. For the two-rope system, we show how the sequence of rope failure depends on how quickly it is applied, highlighting the role of acceleration and inertial effects. In the three-rope system, we identify a critical angle beyond which the upper ropes fail under quasi-static loading.

Beyond theoretical interest, these configurations lend themselves well to classroom demonstrations and laboratory experiments. Using readily available materials, such as identical ropes, spring scales, pulleys, and variable masses, students can recreate the described systems and test the predicted outcomes. In the three-rope system, by varying the angle between ropes, students can observe directly which rope breaks first and can correlate their findings with theoretical predictions. The addition of a mass at the junction point introduces further variables, offering opportunities for experimental design and data analysis.

These experiments not only reinforce elementary physics concepts but also encourage scientific reasoning, model testing, and collaborative problem-solving. We hope this work will trigger the interest of physics teachers and their students at high-school or undergraduate university level.

II. TWO ROPES

Consider a rope suspended from a fixed point, with a mass m attached to its free end. When we attach a second rope to the mass and leave its other end free, we obtain the configuration shown in Fig. 1. Both ropes are identical, mass-less, defect-free, and completely rigid with no elasticity (we will temporarily relax the latter condition and again consider it in the rest of the manuscript). We examine what happens when we pull down the lower rope: which rope breaks first depends on how the force is applied.

As Halliday and Resnick discuss [7], two scenarios emerge. In the first scenario, where the lower rope is pulled rapidly, it breaks while the upper rope remains intact. In the second scenario, with gradual pulling, the upper rope breaks first.

The physics behind these scenarios can be understood by noting that in a real setup we don’t deal with an ideal completely rigid rope. Indeed, the ropes have a finite elasticity and hence upon a rapid pull down, we can assume the mass to be accelerated for a very short time period. At a time instant during that period, one can use the Newton’s second law for the attached mass to write (see Fig. 1):

$$T_1 - T_2 = m(a - g). \quad (1)$$

For the rapid pulling we have $a \gg g$ and hence, $T_1 \gg T_2$. Consider the breaking force threshold, T_B , such that if the tension force exceeds this value, the rope would break. During the rapid pull down, when T_1 reaches the breaking tension T_B , T_2 remains below T_B , causing the lower rope to break.

On the other hand, for gradual pulling there is no acceleration and we have $a \approx 0$. Hereafter, we work in this regime (gradual pulling), and retain our idealization of fully rigid non-elastic ropes. Applying the Newton’s second law for this case, we find:

$$T_2 = T_1 + mg > T_1. \quad (2)$$

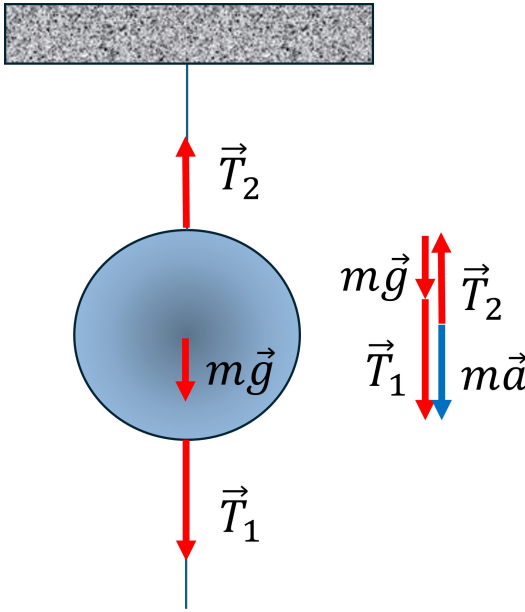


Figure 1. Two-rope configuration: A mass m connects an upper rope (tension T_2) and a lower rope (tension T_1). The forces are also presented in a polygon diagram. The breaking behavior depends on how force is applied to the lower rope. For a rapid pull down, the ropes cannot be considered rigid, and the mass accelerates for a short period of time. However, for a static situation with the force \vec{T}_1 gradually increasing, the acceleration, \vec{a} , vanishes and we assume the ropes to be ideally rigid.

Here, gradually pulling down the lower rope, T_2 reaches T_B first, because it is larger than T_1 , and therefore the upper rope is the one which breaks. As mentioned above, these results assume identical breaking tensions T_B for all ropes.

III. THREE ROPES AND THE CRITICAL ANGLE

The problem becomes more intriguing with three ropes arranged in a Y-shape, as shown in Fig. 2. The upper two ropes form an angle 2θ and connect to a third vertical rope. In what follows we shall only consider the gradual pulling scenario.

Based on intuition and comparing to the previous case, one expects that when the attached mass is small enough (to be more precise, when the gravity force is less than the breaking tension threshold, T_B) and the upper ropes are vertical (i.e., for $\theta = 0^\circ$), always the lower rope breaks. However, the question is, what happens if $\theta > 0^\circ$? This issue is addressed in the following sections.

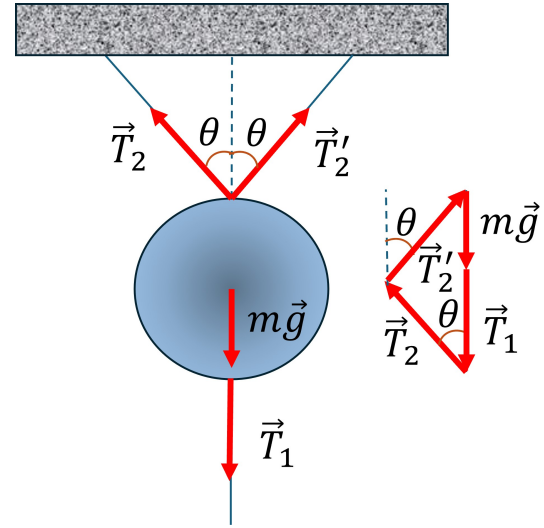


Figure 2. Three-rope Y-configuration with the forces shown in polygon too. The angle 2θ between upper ropes determines which rope breaks first under vertical loading. The value of the tension force in the upper ropes is the same: $T_2 = T_2'$.

A. No mass attached

First, consider a mass-less connection point ($m = 0$). Force balance gives:

$$T_1 - 2T_2 \cos \theta = 0 \quad \text{or} \quad \frac{T_1}{T_2} = 2 \cos \theta. \quad (3)$$

This reveals a critical angle, for which $T_1 = T_2$:

$$\theta_C = \cos^{-1}\left(\frac{1}{2}\right) = 60^\circ. \quad (4)$$

For $\theta < \theta_C$, $\cos \theta > 1/2$ leads to $T_1 > T_2$, so the lower rope breaks first. The extreme case of the vertical upper ropes, $\theta = 0^\circ$ gives $T_1 = 2T_2$, clearly breaking the lower rope, as one would expect.

For $\theta > \theta_C$, $T_1 < T_2$ holds, so the upper ropes break first. This occurs because at larger angles, $\cos \theta < 1/2$ and therefore T_2 is larger than the sum of the vertical components, $2T_2 \cos \theta$. These conclusions are independent of T_B value under our assumptions.

For $\theta = \theta_C$ the three ropes break at the same time in an ideal situation. However, in reality the ropes are not perfectly ideal and because of the defects in the ropes and/or errors in measuring the angles, usually just one of the three ropes breaks.

This shows that in order to break a rope by a small vertical force, one needs to tie up its ends, so that the angle created in the Y-shape is close to 90° and the rope can be broken by a smaller force T_1 . In a real setup though, the ropes have a little bit of elasticity and therefore upon exerting the force T_1 , the angle θ gets smaller. In other words, the elasticity tends to save the upper ropes and instead prefers the lower one to be broken.

One question that can be answered using the above discussion is, what is the maximum force that can be exerted on this system? Or, in other words, what exerted force would break this system? Here, we consider the force to be exerted on the lower rope, and hence, is equal to the its tension. The maximum tension above which the system would break is dubbed $T_1^{(B)}$ in the following. If $\theta < \theta_C$, the lower rope is the one which breaks, and hence, $T_1^{(B)}$ is just equal to the breaking tension, T_B . If $\theta > \theta_C$, the upper ropes break, and hence the maximum exerted force is obtained by letting T_2 reach its maximum value, which is T_B . Setting $T_2 \rightarrow T_B$ in Eq. 3, one obtains $T_1^{(B)} = 2T_B \cos \theta$. This discussion is summarized in the following equation:

$$T_1^{(B)} = \begin{cases} T_B; & \theta < \theta_C, \\ 2T_B \cos \theta; & \theta \geq \theta_C. \end{cases} \quad (5)$$

B. The effects of the attached mass

In the previous section we considered the case where the mass of the junction was negligible. Here, let's consider a case in which a weight is attached to the junction. With mass m at the junction ($m \neq 0$) and gradual pulling ($a = 0$), the balance becomes:

$$\frac{T_1 + mg}{T_2} = 2 \cos \theta. \quad (6)$$

In this case, even if θ is smaller than the critical angle of the zero-mass case, it doesn't necessarily mean the lower rope will break, because the force T_2 should be larger than the zero-mass case to compensate for mg . As such, the critical angle depends on the mass and the breaking tension, T_B . The critical angle, $\theta_{C,m}$, is obtained by setting $T_1 = T_2 = T_B$ in Eq. 6 as

$$\theta_{C,m} = \cos^{-1} \frac{1 + mg/T_B}{2}, \quad (7)$$

which now depends on the value of T_B . Note that if $T_B \gg mg$, we get back to the mass-less case. This indicates that the mass-less contact point is a case in which the weight of the contact point is much less than the breaking tension of the ropes.

Note that the weight mg cannot be infinitely large. The maximum value of the mass for each angle θ is the mass which would just break the upper ropes without any force from the lower rope. Setting $T_1 = 0$ and $T_2 = T_B$ in Eq. 6 we get:

$$\frac{m_{\max}g}{T_B} = 2 \cos \theta. \quad (8)$$

Therefore, noting $\cos \theta \leq 1$, the mass we suspend should be always small enough to satisfy

$$\frac{m_{\max}g}{T_B} < 2. \quad (9)$$

The above discussion clarifies that we have two different regimes, considering the value of $\frac{mg}{T_B}$. The first regime is when $\frac{mg}{T_B} \leq 1$. In such a case, the argument of the inverse-cosine function in Eq. 7 is not larger than unity, and hence the critical angle is well-defined. For $\theta \gtrless \theta_{C,m}$, given that our angles are in the range 0° to 90° , we have $\cos \theta \lessgtr \cos \theta_{C,m}$. Substituting the values of the cosine functions from Eqs. 6 and 7, we get:

$$T_1 + mg \lessgtr T_2 + T_B \frac{mg}{T_B}, \quad \text{for } \theta \gtrless \theta_{C,m}. \quad (10)$$

Let's assume we pull down the system until $T_2 \rightarrow T_B$. For $\theta < \theta_{C,m}$, the inequality 10 implies that $T_1 > T_B$, which is not possible, because the tension in any rope cannot exceed T_B . Consequently, T_2 cannot reach T_B before T_1 does, and hence the lower rope breaks and not the upper ones. On the other hand, if $\theta > \theta_{C,m}$, the inequality 10 implies that $T_1 < T_B$, which means that the upper rope breaks while the lower one remains intact. This argument shows the same concept of the critical angle as the case of the mass-less contact: if the angle θ is smaller than $\theta_{C,m}$, the lower rope breaks first, while if it is larger than $\theta_{C,m}$, the upper ones break first.

Similar to the previous section, we can find the exerted force which would break the system. Clearly, for $\theta < \theta_{C,m}$, we just have $T_1^{(B)} = T_B$, while for $\theta > \theta_{C,m}$ in which case the upper rope breaks, we should set $T_2 \rightarrow T_B$ in Eq. 6. The result is the following:

$$T_1^{(B)} = \begin{cases} T_B; & \theta < \theta_{C,m}, \\ 2T_B \cos \theta - mg; & \theta \geq \theta_{C,m}. \end{cases} \quad (11)$$

The case $\frac{mg}{T_B} = 1$ deserve a specific attention. In this case, Eq. 7 gives $\theta_{C,m} = 0^\circ$. For a non-zero θ , being larger than the critical angle, the above reasonings clarify that the upper ropes break upon pulling down the system. For $\theta = \theta_{C,m} = 0^\circ$, the inequality 10 tells us that if $T_2 \rightarrow T_B$, also $T_1 \rightarrow T_B$, and therefore the three ropes break together, in ideal conditions.

The second regime is when $1 < \frac{mg}{T_B} < 2$. In this regime, the argument of the inverse cosine function in Eq. 7 exceeds unity, and hence we don't have any critical angle. Using Eq. 6 and the fact that $\cos \theta \leq 1$, we get $T_1 + mg \leq 2T_2$. However, in this case, $T_B < mg$ and no tension can exceed T_B , which means $T_1 < mg$, and consequently, $2T_1 \leq T_1 + mg$. Combining the two inequalities we get $T_1 < T_2$, which shows that by exerting the force, the tension in the upper ropes reach T_B first, and independently of angle θ , always the upper ropes break. In short, in this large-mass regime, the upper ropes break.

IV. EXPERIMENTAL RESULTS

To validate our theoretical predictions, we designed a simple experimental setup using cotton strings instead of ropes, as they can be broken with relatively small forces.

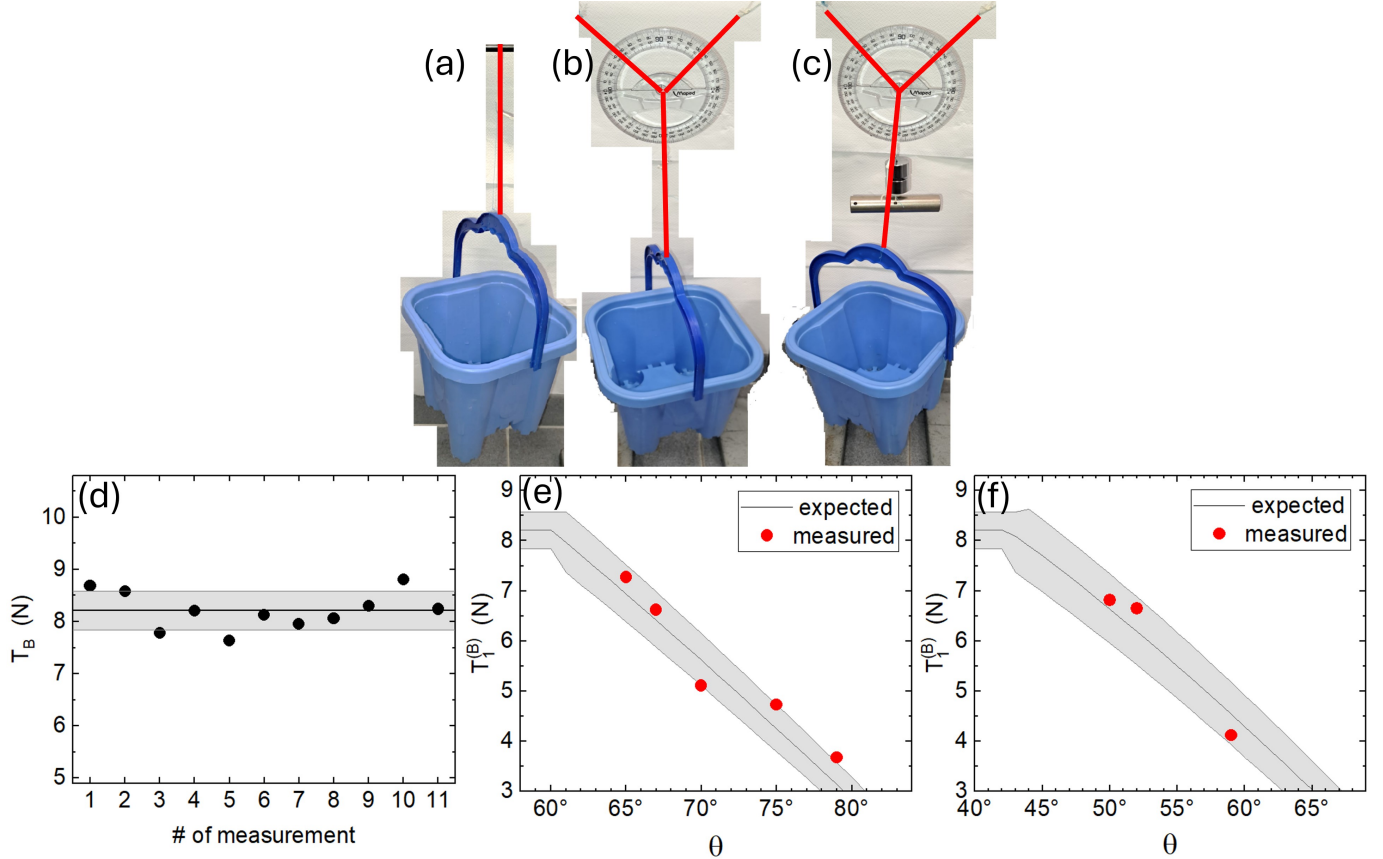


Figure 3. Experimental setup and results. (a) Measurement of breaking tension T_B using a single string. (b) Three-rope case (Y-configuration) without mass at junction for measuring $T_1^{(B)}$. (c) Three-rope case (Y-configuration) with mass $m = 0.400$ kg at the junction. In the panels (a),(b) and (c), the cotton strings are very difficult to be seen as they are very thin, and are therefore marked by thick red lines. Note that, due to the camera perspective, some of the vertical strings may not appear perfectly vertical. (d) Measured T_B values from multiple trials, with gray band showing mean \pm standard deviation. (e) Maximum exerted force, $T_1^{(B)}$, versus angle θ for massless three-rope case ($m = 0$), compared with theoretical prediction (gray band). (f) $T_1^{(B)}$ versus θ for the three-rope case with mass at junction, showing reduced critical angle.

All experiments were conducted under quasi-static loading conditions, with forces applied gradually to ensure negligible acceleration effects.

We first determined the breaking tension, T_B , of individual cotton strings using the setup shown in Fig. 3(a). A bucket was suspended from a single string, and water was poured slowly into the bucket until the string broke. The total weight of the water and bucket at the breaking point was measured to obtain T_B . Multiple measurements were performed to account for statistical variations and potential defects in the strings. As shown in Fig. 3(d), the measured breaking tensions exhibited some scatter, with a mean value of $T_B = 8.2 \pm 0.4$ N, represented by the gray band (the value ± 0.4 N is calculated from the standard deviation). We found that careful, slow pouring was essential to obtain consistent results, and measurements yielding significantly lower T_B values (attributed to string defects) were excluded from the analysis.

Next, we investigated the three-rope Y-configuration

without mass at the junction ($m = 0$), as depicted in Fig. 3(b). For various fixed angles θ , water was gradually added to the bucket until one of the strings broke. The angle θ was measured precisely at the moment of string breaking. Our experiments confirmed the theoretical prediction: for $\theta < \theta_C = 60^\circ$, the lower rope consistently broke first, while for $\theta > \theta_C$, one of the upper ropes failed (with the specific upper rope breaking depending on minor defects and little angular asymmetries). The measured maximum exerted force, $T_1^{(B)}$, for $\theta > \theta_C$ is plotted in Fig. 3(e), showing good agreement with the theoretical expectation from Eq. 5. The theoretical expectation is obtained by using the value $T_B = 8.2$ N in Eq. 5. The upper limit of the theoretical expectation is obtained by using the upper limit of T_B , which is $8.2 + 0.4$ N, and the angle $\theta \rightarrow \theta - \Delta\theta$ in Eq. 5 (note that $\cos \theta$ is a decreasing function in this range). The lower limit is obtained by using $T_B \rightarrow 8.2 - 0.4$ N and $\theta \rightarrow \theta + \Delta\theta$ in Eq. 5. The error of the angle measurement is considered to be $\Delta\theta = 1^\circ$. The area between the upper and lower the-

oretical expectations is shaded gray. We note that due to the slight elasticity of the cotton strings, the angle θ decreased gradually during loading, requiring careful measurement at the instant at which the strings break.

Finally, we examined the case with mass $m = 0.400$ kg attached at the junction point, using the same three-rope setup shown in Fig. 3(c). According to Eq. 11, this additional mass reduces the critical angle to $\theta_{C,m} \simeq 42^\circ$, significantly lower than the mass-less case. Therefore, we focused our measurements on angles below 60° to clearly demonstrate this shift. The experimental results for $T_1^{(B)}$, shown in Fig. 3(f), agree well with the theoretical prediction from Eq. 11 (gray band, obtained through a similar procedure to the one of panel (e), but using Eq. 11), confirming that the presence of mass at the junction alters the breaking behavior as predicted.

SUMMARY

In this work, we show that by studying the distribution of tension and the conditions for rope failure in idealized multi-rope systems, a deeper insight into Newton's law can be attained.

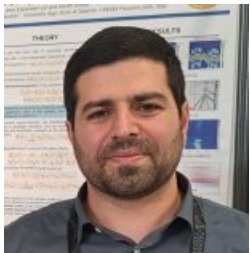
Beginning with a simple two-rope vertical configuration, where a body of mass m is sustained by a vertical

tension \vec{T}_2 and is pulled downward by applying a tension \vec{T}_1 to it. In this case we show that the rate at which the pulling force is applied, suddenly or gradually, determines whether the upper or lower rope breaks. The same analysis is extended to a three-rope Y-configuration system, for which we may identify a critical angle θ_C beyond which the failure shifts from the lower to the upper ropes. We further examine how the introduction of mass at the junction point alters the critical angle and imposes mass-dependent limits on the system stability.

These scenarios, though analyzed under ideal assumptions (mass-less, rigid ropes and uniform breaking tension), mirror real-world behaviors when adjusted for elasticity and damping. More importantly, they offer opportunities to implement laboratory activities. In fact, the rope-breaking phenomena can be reproduced and tested through hands-on experiments. On their turn, these activities may foster inquiry, model-based reasoning, and deeper understanding of Newtonian mechanics. To clearly demonstrate one example of such activities, we conceived an experimental setup and performed some measurements and showed their agreement with the theoretical formulas within experimental errors.

Therefore, by blending analytical modeling with engaging experimental activities, this work may serve as a resource for educators aiming to connect elementary physics principles with active learning.

- [1] Y. Guo, D. Zhang, X. Zhang, S. Wang, and W. Ma, *Shock and Vibration* **2020**, 8506016 (2020).
- [2] M. Chen and Y. He, *Information Technology and Control* **50**, 752 (2021).
- [3] S. Mao, J. Tao, J. Xie, S. Xu, L. Chen, H. Yu, and C. Liu, *Journal of Low Frequency Noise, Vibration and Active Control* **42**, 1055 (2023).
- [4] S. Xu, J. Tao, C. Dong, S. Mao, J. Xie, and C. Liu, *Proceedings of the Institution of Mechanical Engineers, Part C: Journal of Mechanical Engineering Science* **237**, 2316 (2023).
- [5] Y. Zhang, G. Cao, and G. Wang, *IEEE Transactions on Instrumentation and Measurement* **72**, 1 (2023).
- [6] S. Flores-Garcia, L. Alfaro-Avena, J. Chávez-Pierce, J. Luna-González, and M. González-Quezada, *American Journal of Physics* **78**, 1412 (2010).
- [7] D. Halliday, R. Resnick, and J. Walker, *Fundamentals of Physics*, 10th ed. (Wiley, 2014).

Amir Eskandari-asl

Amir Eskandari-asl, born on January 30, 1987, earned his Ph.D. in Condensed Matter Physics from Shahid Beheshti University, Tehran, Iran, in 2017. He is currently a post-doctoral researcher at the University of Salerno, Italy, where he works on theoretical condensed matter physics with a focus on ultrafast phenomena, light-matter interaction, and out-of-equilibrium quantum dynamics. He has extensive teaching experience at both undergraduate and graduate levels, including courses in Non-Equilibrium Physics, Solid State Physics, Mathematical Physics, and Basic Physics. He has authored several research papers in condensed matter theory and contributed to physics education through publications such as his work on the static properties of Slinky. His research contributions include the development of theoretical frameworks for understanding pumped quantum systems and quantum transport in nanoscale devices.

Roberto De Luca

Roberto De Luca, born on June 8, 1958, earned a degree in physics from the University of Salerno, Italy, in 1986. He received his MA in physics from the University of Southern California in 1987 and his PhD from the University of Naples and Salerno in 1992. Since 1994, he has been conducting research at the University of Salerno. His original research focused on Josephson junction array models and the dynamics of superconducting devices. Since 2001, he has authored papers on physics education. Some of his works in this field have been dedicated to finding simple ways to introduce alternative energy concepts to young students.